Isobaric Vapor–Liquid Equilibrium Data for Six Binary Systems: Prop-2-en-1-ol (1)–Hexan-2-ol (2), Prop-2-en-1-ol (1)–Hexan-2-one (2), Hexan-2-one (1)–Hexan-2-ol (2), Prop-2-en-1-ol (1)–4-Methyl-pentan-2-ol (2), Prop-2-en-1-ol (1)–4-Methyl-pentan-2-one (2), and 4-Methyl-pentan-2-one (1)–4-Methyl-pentan-2-ol (2) at 101.32 kPa

Karen Silva[1*], Marcia Araque[1], Benjamin Katryniok[1]

[1] Univ. Lille, CNRS, Centrale Lille, ENSCL, Univ. Artois, UMR 8181 - UCCS - Unité de Catalyse et Chimie du Solide, F-59000 Lille, France

*Corresponding Author:

Keywords:

Vapor-liquid equilibrium, Allyl alcohol, 2-hexanol, MIBC, UNIQUAC Model

Abstract.

In this work, the Isobaric vapor-liquid equilibrium (VLE) measurements were conducted for the binary systems of Allyl alcohol/2-hexanol, Allyl alcohol/2-hexanon e, 2-hexanone/2-hexanol, Allyl alcohol/MIBC, Allyl alcohol/MIBK, and MIBK/MIBC to assist with the design of the separation process by distillation. Measurements were determined by Fischer VLE 602 equipment at 101.32 kPa. The thermodynamic consistency of the measured VLE data was validated by Herington (Wisniak criterion), Van Ness, pure component consistency and Redlich-Kister total area tests. Moreover, data sets were correlated using the non-random two-liquid (NRTL), universal quasichemical (UNIQUAC) and Wilson thermodynamic models to obtain the binary interaction parameters using Aspen Plus commercial software. The root-mean-square deviation (RMSD) of equilibrium temperature (T) and vapor mole fraction (y_i) were less than 0.24 and 0.0089, respectively, which indicate that this three thermodynamic models can be used to correlate the six binary systems and therefore they can be employed for the development and optimization of the separation process.

1. INTRODUCTION

The Deoxydehydration (DODH) of glycerol is an alternative and sustainable reaction, for the synthesis of allyl alcohol which has recently gained much attention [1][2][3][4]. Generally, a DODH reaction removes two adjacent hydroxyl groups from vicinal diols to afford the corresponding alkene, in the current case, allyl alcohol from glycerol [5][6]. This reaction is typically catalyzed by rhenium based catalyst and requires a stoichiometric reductant such as H_2 or a secondary alcohol[7]. The reductant-solvent acts as hydrogen donor and become oxidized to the corresponding ketone and water is also produce. Considering the application of allyl alcohol as a monomer in the chemical industry, it is imperative to isolate it in high purity from the reaction mixture containing the solvent, the co-produced ketone and water. Hence, in order to develop separation and purification strategies for allyl alcohol from the DODH of glycerol, high precision experimental phase equilibrium data are required [8][9]**.**

The Vapor-liquid equilibrium of allyl alcohol/water is already reported in the literature [10] and vapor-liquid-liquid equilibrium of solvent/water and ketone/water binary systems are in Aspen database. Thus, this work focuses on the experimental measuring of VLE data for the binary mixtures of Allyl alcohol/2-hexanol, Allyl alcohol/2-hexanone, 2-hexanone/2-hexanol, Allyl alcohol/MIBC, Allyl alcohol/MIBK, and MIBK/MIBC at 101.32 kPa, in order to calculate the adjustable binary interaction parameters from local-composition models[11]. In order to validate the accuracy and quality of the VLE data, the Herington[12][13], Van Ness[14] pure component consistency[15] and Redlich-Kister[16] total area tests were implemented to verify the thermodynamic consistency of VLE data sets before fitting using the universal quasichemical (UNIQUAC) [17], non-random two-liquid (NRTL) [18] and Wilson[19] thermodynamic models.

2. EXPERIMENTAL SECTION

2.1. Materials

All of the experimental chemicals used in this study are listed in Table 1 . The masse fraction reported by the manufacturer was confirmed by gas chromatographic analysis (GC) equipped with a flame ionization detector (FID), using the area method. Furthermore, a comparison between measured boiling temperatures and reported values from literature was carried out. As given in Table 1, close values were noted; the maximum boiling point deviation for Allyl alcohol, 2-hexanol, 2-hexanone, MIBC and MIBK are 0.23 K, 0.27K, 0.58K, 0.1K and 0.17K, respectively.

Table 1. Experimental components information.

Component	CAS	Suppliers	Mass fraction	T_b [K][a]		Analysis method
				This work	Lit	
Allyl Alcohol	107-18-6	Sigma-Aldrich	≥ 0,990	369.98	369.75 [10] 370.07 [20] 369.94 [21]	GC[b]
2-hexanol	626-93-7	Sigma-Aldrich	≥0,990	412.77	413.04 [22][23]	GC[b]
2-hexanone	591-78-6	Acros Organics	≥0,980	400.12	400.7[23]	GC[b]
4-methyl-2-pentanol (MIBC)	108-11-2	Sigma-Aldrich	≥ 0,980	404.75	404.85[23]	GC[b]
4-methyl-2-pentanone (MIBK)	108-10-1	Sigma-Aldrich	≥ 0.995	388.83	389[23]	GC[b]

[a] The experimental pressure for the measurement of boiling temperature is 101.32 kPa; standard uncertainties of experimental pressure and temperature are $u(T_b)$ = 0.1K $u(P)$ = 0.1 kPa. [b]Gas chromatography.

2.2. VLE apparatus and procedure

The binary VLE data were determined using an equilibrium apparatus Fischer VLE 602 equipped with a Cottrell circulation pump (Figure 1). Accuracy in measurements of temperature and pressure are ±0.1 K and 0.1 kPa, respectively. The operation procedure is based on the principle of circulation method, to ensure an intimate contact between liquid and vapor phases during the boiling

process. At the beginning, the mixed chamber (5) and the side reservoir (1) are loaded with the less volatile pure component, then, different binary mixtures were prepared as needed by controlled addition of the second component to the equilibrium chamber via liquid-phase septum (11). For each equilibrium point, the pressure was fixed and the heating and stirring systems were turned on. The heating supply is adapted so that the reflux flow of the vapor phase is 1-2 drops per second. The apparatus was operated at constant pressure until equilibrium was reached. Equilibrium condition is assumed when temperature variations are less than 0.1 K for at least 30 min at constant pressure. The temperature and pressure variations are monitored in real time by statistical control charts. Once the equilibrium condition attainted, samples of liquid and condensed vapor were taken for gas chromatography analysis. All experiments were carried out at 101.13 kPa of pressure. Between 15 to 22 equilibrium points were generated for each binary system. To verify the performance of the apparatus, vapor pressure data of pure components were also measured, and the coefficients of Antoine extended equation were fitted. Approximately 18 to 20 equilibrium points for each pure component were measured.

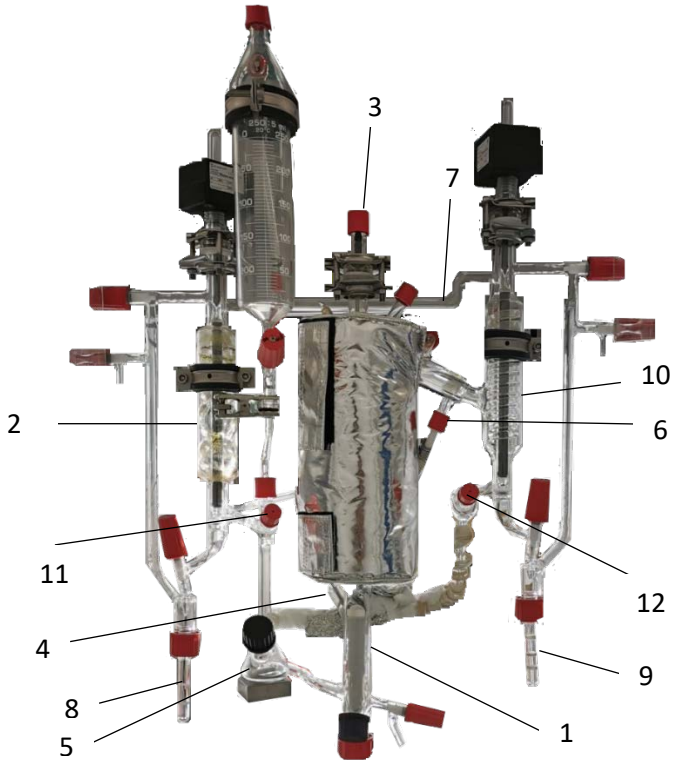

Figure 1. Apparatus Fisher VLE 602 used in this work. 1: Reservoir with immersed rod heater. 2: Condenser. 3: Vapor-phase temperature sensor. 4: Liquid-phase temperature sensor. 5: Mixer chamber. 6: Coolant water connection. 7: Pressure control line. 8: Liquid sampling port. 9: Vapor sampling port. 10: Condenser. 11: Liquid-phase septum. 12: Vapor-phase septum.

2.3. Sample Analysis

The concentrations of Liquid and condensed vapor samples were determined by gas chromatography using a GC instrument equipped with a column CP-Wax52CB (30m x 250 µm x 0.25 µm) and a flame ionization detector (FID). The initial oven temperature was programmed at 40°C for 2 min, with a heating ramp of 10°C/min, up to 100°C. The injection port temperature was maintained at 250°C using split injection mode adjusted to 140:1 ratio. In each analysis, 1µL of sample was injected.

VLE samples of 20 µL were diluted in 980 µL of Tetrahydrofuran (THF). 20 µL of benzene was added in each sample as internal standard. The uncertainty in the concentration measurements was determined by analyzing solutions with known composition, using the calibration curves of the chromatographic technique to this end. Ten calibration standards were prepared gravimetrically per each binary system. A maximum standard uncertainty of ± 0.001 in the mole fraction of each component was estimated.

3. RESULTS AND DISCUSSION

3.1. Vapor pressure correlation of pure components

Despite the availability of vapor pressure data for Allyl alcohol, 2-hexanol, 2-hexanone, MIBC and MIBK in Aspen physical properties database, measurement of the vapor pressure for this components was performed, bearing in mind that this information is fundamental for a proper application of the consistency tests [26] as well as checking the reliability of the equilibrium apparatus used in this work. The experimental vapor pressures of the components are present in Table 2. Numerical data regression was carried out to fit the vapor pressure data with Extended Antoine equation (Eq 1) and the corresponding coefficients are presented in Table 3. A maximum average error of 0.004 kPa between experimental and calculated vapor pressures was observed. As showed in Figure 2, vapor pressure data also agree with the values previously reported (NIST database).

Table 2. Measured vapor pressure data for all components

Pressure (kPa)	Temperature (K)				
	Allyl alcohol	2-hexanol	2-hexanone	MIBC	MIBK
101.32	369.98	412.77	400.12	404.75	388.83
95	368.22	410.51	397.64	402.78	386.61
90	366.78	408.88	395.78	401.14	384.78
85	365.27	407.15	393.9	399.45	382.87
80	363.69	405.28	391.87	397.66	380.88
75	362.01	403.41	389.82	395.78	378.76
70	360.26	401.41	387.53	393.82	376.53
65	358.39	399.28	385	391.73	374.18
60	356.38	397.16	382.49	389.5	371.68
55	354.26	394.65	379.79	387.14	368.98
50	351.96	391.98	376.8	384.6	366.11
45	349.43	389.21	373.75	381.84	363
40	346.68	386.15	370.49	378.83	359.58
35	343.63	382.61	366.59	375.5	356
30	340.2	378.87	362.37	371.76	351.57
25	336.23	374.64	357.44	367.48	346.71
20	331.54	369.48	351.06	362.46	341

[a] u(T) =0.036K and u(P)=0.004 kPa

$$Ln\left(P_i^s/_{kPa}\right) = C_1 + \frac{C_2}{T + C_3} + C_4 T + C_5 Ln(T) + C_6 T^{C_7} \;\; for \;\; C_8 \leq T \leq C_9 \qquad \text{Eq 1}$$

Table 3. Coefficients of the extended Antoine equation

Component	C_1	C_2	C_3	C_4	C_5	C_6	C_7	C_8/K	C_9/K
Allyl Alcohol	77.91	-7702.23	-10.25	-0.0011	-8.72	1.83E-16	5.78	144.15	545.1
2-hexanol	109.31	-8191.02	-47.58	-0.0032	-13.65	4.32E-06	2.09	223	585.3
2-hexanone	100.13	-9625.98	26.73	0.0062	-12.64	5.26E-06	1.82	217.35	587.61
4-methyl-2-pentanol (MIBC)	66.27	-4160.32	-98.28	0.0095	-8.65	8.07E-16	4.82	183	574.4
4-methyl-2-pentanone (MIBK)	72.26	-8325.25	36.24	0.0075	-8.52	-1.63E-16	5.82	189.15	574.6

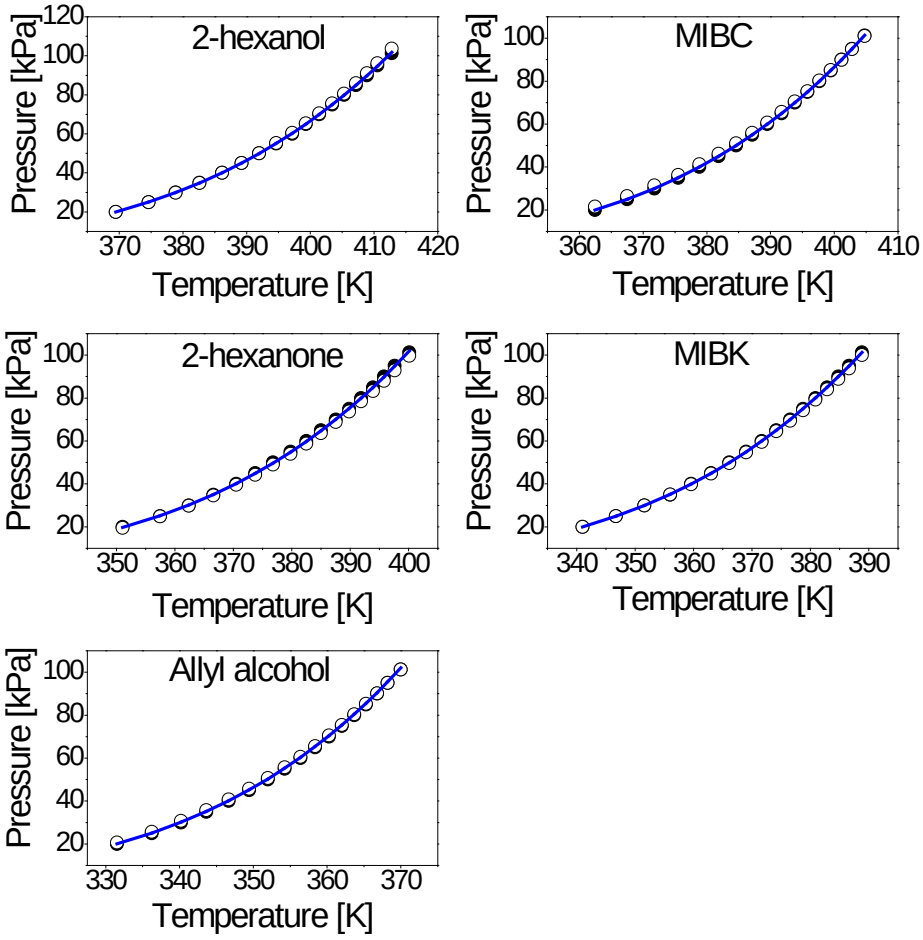

Figure 2. Vapor pressure for 2-hexanol, MIBC, 2-hexanone, MIBK and Allyl alcohol. The continuous blue line denotes the Antoine equation with regressed parameters. (●) represents experimental data and (○) reported data from the NIST database.

3.2. Vapor-liquid equilibrium (VLE) model

VLE experimental data for the binary systems were used to calculate the activity coefficients (γ_i). The VLE relationship at moderate pressure can be expressed as showed in Eq 2 [27]. Due to the fact that the experimental data was obtained at low pressure (101.32 kPa), vapor phase behaviour was considered as ideal gas, and therefore, fugacity coefficient (φ_i^v) and pointing factor were fitted to one [28]. Thus, VLE expression can be simplified as showed in Eq 3. Where x_i and y_i are the composition of the liquid and vapor phases, respectively, P is the total system pressure. P_i^s is the vapor pressure of pure component i at the system temperature. P_i^s was calculated using the Antoine coefficients

previously fitted with our experimental data. Experimental VLE data with the corresponding experimental activity coefficients are listed in Table 4-6.

$$Py_i\varphi_i^v = P_i^s\varphi_i^s\gamma_i x_i \exp\int_{P_i^s}^{P} V_i^l dp \ (i = 1.2.3. \ldots . N) \quad \text{Eq 2}$$

$$\gamma_i = \frac{y_i P}{x_i P_i^s} \quad \text{Eq 3}$$

To evaluate the ideality deviations of the systems under the same composition and pressure conditions, excess Gibbs energy (G^E) was determined by Eq 4 [9], where R is the universal gas constant, and T is the system temperature. Taking into account that γ_1 and G^E values are above unity and zero (Table 4-6), respectively. Positive deviations for all binary systems are evidenced. G^E for the six binaries have been correlated by a sixth order polynomial equation and plotted in Figure 3. The mixtures of Allyl alcohol/2-hexanone and Allyl alcohol/MIBK showed the biggest nonideality from Raoul's law compared to those of the other four mixtures. The largest value of the G^E is observed when the mixture have equal mole fraction in allyl alcohol and corresponding ketone. Taking all systems, G^E follow the order Allyl alcohol/2-hexanone > Allyl alcohol/MIBK > MIBK/MIBC > 2-hexanone/2-Hexanol > Allyl alcohol/2-Hexanol > Allyl alcohol/MIBC.

$$G^E = RT\ (x_1 Ln\gamma_1 + x_2 Ln\gamma_2) \quad \text{Eq 4}$$

Table 4. Isobaric Vapor-liquid equilibrium data for Allyl alcohol/2-hexanol and Allyl alcohol/MIBC systems at 101.32 kPa

Allyl alcohol (1)/2-hexanol (2)							Allyl alcohol (1)/MIBC (2)						
T(K)	x_1	y_1	γ_1	γ_2	$Ln\left(\frac{\gamma_1}{\gamma_2}\right)$	$G^{E\ (a)}$	T(K)	x_1	y_1	γ_1	γ_2	$Ln\left(\frac{\gamma_1}{\gamma_2}\right)$	$G^{E\ (a)}$
412.62	0	0		1.0003			404.74	0	0		1.0002		
412.02	0.0060	0.0247	1.0467	1.0003	0.0454	1.789	403.51	0.0181	0.0570	1.0290	0.9999	0.0287	1.537
410.84	0.0183	0.0727	1.0451	0.9998	0.0443	2.212	402.15	0.0386	0.1170	1.0321	1.0001	0.0315	4.363
408.62	0.0422	0.1576	1.0482	1.0001	0.0470	7.210	401.9	0.0426	0.1280	1.0309	1.0000	0.0304	4.363
406.88	0.0622	0.2207	1.0484	1.0004	0.0468	11.236	399.76	0.0768	0.2170	1.0350	1.0003	0.0342	9.584
404.09	0.0965	0.3158	1.0508	1.0006	0.0490	17.865	398.03	0.1063	0.2850	1.0361	1.0006	0.0349	14.099
400.69	0.1425	0.4207	1.0510	1.0026	0.0472	30.980	395.82	0.1465	0.3670	1.0374	1.0008	0.0359	19.959
396.98	0.1989	0.5246	1.0532	1.0033	0.0485	42.636	393.51	0.1917	0.4466	1.0380	1.0017	0.0356	27.801
394.72	0.2369	0.5826	1.0544	1.0030	0.0499	48.707	390.77	0.2506	0.5340	1.0368	1.0032	0.0329	37.196
391.78	0.2910	0.6514	1.0542	1.0044	0.0484	60.063	389.45	0.2808	0.5734	1.0371	1.0038	0.0326	42.028
389.74	0.3320	0.6955	1.0540	1.0051	0.0475	67.466	387.47	0.3295	0.6296	1.0357	1.0053	0.0297	48.698
386.16	0.4130	0.7657	1.0495	1.0094	0.0390	81.718	385.00	0.3961	0.6947	1.0321	1.0089	0.0227	57.146
383.2	0.4890	0.8180	1.0460	1.0119	0.0332	89.235	383.93	0.4268	0.7213	1.0310	1.0104	0.0201	60.521
381.79	0.5290	0.8410	1.0430	1.0147	0.0274	92.511	381.38	0.5058	0.7807	1.0269	1.0170	0.0097	69.022
379.92	0.5860	0.8691	1.0376	1.0253	0.0119	101.042	380.34	0.5405	0.8035	1.0251	1.0206	0.0044	71.921
377.70	0.6610	0.9010	1.0303	1.0378	-0.0073	101.523	378.47	0.6076	0.8429	1.0207	1.0285	-0.0076	73.928
376.8	0.6940	0.9130	1.0264	1.0491	-0.0219	102.564	377.05	0.6639	0.8718	1.0155	1.0371	-0.0210	70.376
374.29	0.7940	0.9460	1.0163	1.0758	-0.0569	86.846	375.65	0.7228	0.8990	1.0107	1.0482	-0.0365	64.817
373.00	0.8510	0.9620	1.0101	1.1064	-0.0911	73.310	374.41	0.7772	0.9219	1.0075	1.0608	-0.0516	59.029
371.87	0.9040	0.9760	1.0051	1.1392	-0.1252	52.905	373.35	0.8257	0.9408	1.0053	1.0737	-0.0658	52.136
370.79	0.9570	0.9890	1.0008	1.2223	-0.1999	28.998	371.99	0.8919	0.9647	1.0026	1.0924	-0.0858	36.601
369.91	1	1	1.0003				370.94	0.9459	0.9827	1.0006	1.1180	-0.1109	20.330
							369.89	1	1	1.0010			

Table 5. Isobaric Vapor-liquid equilibrium data for Allyl alcohol/2-hexanone and Allyl alcohol/MIBK systems at 101.32 kPa

Allyl alcohol (1)/2-hexanone (2)	Allyl alcohol (1)/MIBK (2)

T(K)	x_1	y_1	γ_1	γ_2	$Ln\left(\frac{\gamma_1}{\gamma_2}\right)$	$G^{E\ (a)}$	T(K)	x_1	y_1	γ_1	γ_2	$Ln\left(\frac{\gamma_1}{\gamma_2}\right)$	$G^{E\ (a)}$
399.90	0.0000	0.0000		1.0001			388.84	0.0000	0.0000		1.0000		
398.93	0.0120	0.0390	1.2214	1.0004	0.1996	9.205	388.01	0.0152	0.0388	1.3592	0.9997	0.3072	14.079
397.31	0.0330	0.1020	1.2216	1.0012	0.1990	25.519	387.10	0.0330	0.0807	1.3418	0.9998	0.2942	30.609
395.65	0.0560	0.1650	1.2267	1.0012	0.2031	41.389	385.17	0.0750	0.1659	1.2943	1.0036	0.2544	72.486
392.69	0.1010	0.2700	1.2227	1.0037	0.1973	77.191	383.41	0.1190	0.2418	1.2615	1.0092	0.2232	113.854
390.87	0.1320	0.3320	1.2198	1.0050	0.1937	99.187	381.91	0.1619	0.3142	1.2680	1.0038	0.2336	132.065
388.70	0.1730	0.4020	1.2095	1.0089	0.1813	130.090	380.47	0.2091	0.3786	1.2429	1.0068	0.2107	160.820
386.63	0.2170	0.4670	1.1994	1.0125	0.1693	158.190	379.09	0.2596	0.4389	1.2174	1.0130	0.1838	191.138
384.73	0.2630	0.5250	1.1854	1.0174	0.1528	183.702	377.92	0.3097	0.4955	1.2001	1.0129	0.1696	205.224
382.45	0.3260	0.5910	1.1628	1.0296	0.1217	218.965	376.85	0.3608	0.5429	1.1719	1.0246	0.1343	228.039
380.21	0.3990	0.6530	1.1336	1.0527	0.0740	255.730	375.98	0.4070	0.5842	1.1528	1.0324	0.1103	240.064
378.20	0.4770	0.7100	1.1056	1.0793	0.0240	276.010	375.02	0.4643	0.6263	1.1210	1.0587	0.0572	260.579
376.40	0.5590	0.7620	1.0786	1.1146	-0.0327	282.111	374.22	0.5177	0.6618	1.0932	1.0915	0.0016	274.909
375.16	0.6240	0.7990	1.0588	1.1504	-0.0830	275.566	373.47	0.5737	0.7056	1.0805	1.1009	-0.0187	265.246
374.04	0.6900	0.8350	1.0416	1.1892	-0.1325	254.436	372.84	0.6256	0.7382	1.0605	1.1374	-0.0700	263.402
373.17	0.7460	0.8640	1.0286	1.2318	-0.1803	229.487	372.30	0.6774	0.7733	1.0463	1.1631	-0.1058	245.714
372.36	0.8020	0.8930	1.0183	1.2778	-0.2270	195.251	371.79	0.7266	0.8076	1.0378	1.1841	-0.1319	226.037
371.79	0.8440	0.9150	1.0122	1.3135	-0.2605	163.192	371.42	0.7692	0.8351	1.0274	1.2166	-0.1690	204.015
371.09	0.8990	0.9440	1.0058	1.3689	-0.3082	113.867	371.05	0.8188	0.8667	1.0154	1.2678	-0.2220	171.138
370.82	0.9210	0.9560	1.0041	1.3879	-0.3236	91.507	370.69	0.8705	0.9020	1.0072	1.3195	-0.2701	129.796
370.41	0.9560	0.9750	1.0016	1.4358	-0.3602	53.581	370.15	0.9520	0.9613	1.0012	1.4307	-0.3570	56.280
369.91	1.0000	1.0000	1.0003				369.90	1.0000	1.0000	1.0006			

Table 6. Isobaric Vapor-liquid equilibrium data for 2-Hexanone/2-hexanol and MIBK/MIBC systems at 101.32 kPa

2-Hexanone (1)/2-hexanol (2)							MIBK (1)/MIBC (2)						
T(K)	x_1	y_1	γ_1	γ_2	$Ln\left(\frac{\gamma_1}{\gamma_2}\right)$	$G^{E\ (a)}$	T(K)	x_1	y_1	γ_1	γ_2	$Ln\left(\frac{\gamma_1}{\gamma_2}\right)$	$G^{E\ (a)}$
412.62	0.0000	0.0000		1.0003			404.75	0.0000	0.0000		0.9999		
412.46	0.0079	0.0129	1.1497	1.0003	0.1392	4.731	404.33	0.0179	0.0311	1.1364	1.0001	0.1278	7.957
411.87	0.0388	0.0610	1.1268	1.0007	0.1187	18.034	403.89	0.0370	0.0631	1.1299	1.0005	0.1217	16.634
411.04	0.0851	0.1281	1.1036	1.0023	0.0963	35.890	403	0.0771	0.1273	1.1196	1.0012	0.1118	32.827
409.92	0.1509	0.2165	1.0843	1.0060	0.0749	58.956	402.19	0.1150	0.1841	1.1088	1.0025	0.1007	47.217
409.16	0.2010	0.2774	1.0648	1.0105	0.0523	71.399	401.31	0.1575	0.2450	1.1027	1.0034	0.0943	60.894
407.96	0.2820	0.3722	1.0523	1.0159	0.0352	87.314	400.53	0.1966	0.2980	1.0969	1.0042	0.0883	71.749
407.03	0.3490	0.4449	1.0428	1.0215	0.0206	96.298	399.7	0.2410	0.3525	1.0821	1.0082	0.0708	83.669
406.36	0.4010	0.4976	1.0341	1.0273	0.0066	99.789	398.67	0.2964	0.4190	1.0751	1.0104	0.0620	95.377
405.75	0.4510	0.5449	1.0240	1.0360	-0.0116	101.701	397.88	0.3400	0.4682	1.0699	1.0129	0.0547	103.874
404.82	0.5256	0.6172	1.0214	1.0403	-0.0183	100.627	397.05	0.3894	0.5193	1.0597	1.0182	0.0400	110.827
404.20	0.5790	0.6647	1.0161	1.0484	-0.0313	97.920	396.95	0.3970	0.5253	1.0543	1.0216	0.0314	111.866
403.35	0.6555	0.7313	1.0113	1.0567	-0.0439	88.430	396.25	0.4370	0.5666	1.0530	1.0234	0.0285	117.343
402.66	0.7189	0.7837	1.0077	1.0670	-0.0571	79.523	396.15	0.4450	0.5724	1.0475	1.0279	0.0190	118.276
401.92	0.7903	0.8408	1.0043	1.0799	-0.0726	65.153	395.25	0.5050	0.6262	1.0351	1.0394	-0.0042	120.146
401.53	0.8299	0.8716	1.0025	1.0880	-0.0819	54.774	394.4	0.5586	0.6757	1.0338	1.0418	-0.0077	120.047
400.79	0.9060	0.9299	1.0006	1.1029	-0.0973	32.491	393.65	0.6120	0.7192	1.0255	1.0536	-0.0271	116.671
400.37	0.9500	0.9630	1.0002	1.1091	-0.1033	17.998	392.85	0.6700	0.7654	1.0194	1.0647	-0.0435	109.563
399.89	1.0000	1.0000	1.0004				392.1	0.7258	0.8085	1.0152	1.0742	-0.0566	99.611
							391.3	0.7874	0.8532	1.0100	1.0929	-0.0789	87.063
							390.68	0.8380	0.8892	1.0067	1.1070	-0.0950	71.534
							389.99	0.8968	0.9296	1.0029	1.1320	-0.1211	49.974
							389.51	0.9387	0.9582	1.0013	1.1515	-0.1397	31.917
							388.87	1.0000	1.0000	0.9991			

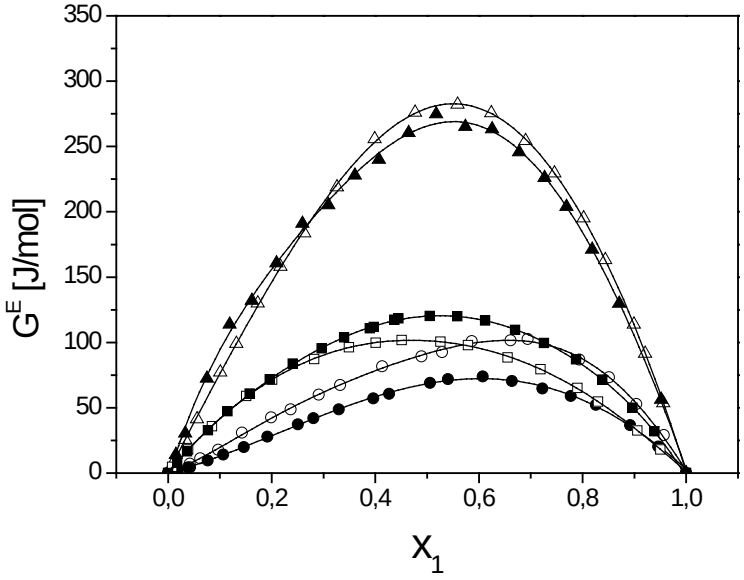

Figure 3. Excess free energies of mixing (G^E) of six binaries at 101.32 kPa. (○) Allyl alcohol/2-hexanol (●) Allyl alcohol/MIBC (Δ) Allyl alcohol/2-hexanone (▲) Allyl alcohol/MIBK (□) 2-hexanone/2-Hexanol (■) MIBK/MIBC, (—) Corresponding polynomial adjustment.

3.3. Thermodynamic consistency test

Thermodynamic consistency tests allow the assessment of experimental VLE data on the basis of Gibbs-Duhem equation (Eq 5-6) [15][26]. The use of several consistency tests is always recommended to check - in the proper manner - the quality of the data, given that, contradictory consistency results can inform one about an incorrect application of a particular test [26]. In this work, Redlich-Kister total area test, Herington test, Modified Herington test by Wisniak and Van Ness test were employed.

$$\sum_i x_i d\bar{M}_i - \left(\frac{dM}{dP}\right)_{x,T} dP + \left(\frac{dM}{dT}\right)_{x,T} dT = 0 \ , \quad M = \frac{G^E}{RT} = \sum_i x_i ln\gamma_i \qquad \text{Eq 5}$$

$$\sum_i x_i dln\gamma_i - \frac{V^E}{RT} dP + \frac{H^E}{RT^2} dT = 0 \qquad \text{Eq 6}$$

Redlich-Kister total area test (1948) assumed the volume and heat effects of mixing (ε) are negligible[13] (Eq 7 - 8). According with Kang et al. [15], a polynomial relation with the form presented in Eq 9, with n , between 4 and 6, can be used for regressing data $Ln\left(\frac{\gamma_1}{\gamma_2}\right)$. Nevertheless, due to the absence at the infinite dilution zones, as reported by Duran et al. [8], Margules Activity Model was used in the pure components zones. The corresponding parameters A_{12} and A_{21}, were obtained by the data regression of Excess Gibbs energy of a binary system[29] (Eq 10), the values were summarized in Table 7. According with Kojima et al [16], for $|A^*| < 0.03$, the test is passed. In addition, the tool for thermodynamic consistency available in Aspen Plus V9 was used[30]. This latter is quite similar to Redlich-Kister area test [8][16][30].

$$A^* = \int_0^1 ln\frac{\gamma_1}{\gamma_2}dx + \int_0^1 \varepsilon\, dx \quad , \quad \varepsilon = -\left(\frac{H^E}{RT^2}\right)\left(\frac{\partial T}{\partial x_1}\right)_P,\ \varepsilon = -\left(\frac{V^E}{RT}\right)\left(\frac{\partial p}{\partial x_1}\right)_T \qquad \text{Eq 7}$$

$$A^* = \int_0^1 ln\frac{\gamma_1}{\gamma_2}dx \qquad \text{Eq 8}$$

$$Ln\left(\frac{\gamma_1}{\gamma_2}\right) = a_n x_1^n + a_{n-1}x_1^{n-1} + \cdots + a_1 x_1 + a_0 \qquad \text{Eq 9}$$

$$\frac{G^E}{RTx_1x_2^2} = A_{21}\frac{x_1}{x_2} + A_{12} \quad , \ \lim_{x_1\to 0}\ln\gamma_1^{\infty} = A_{12}\,,\,, \lim_{x_2\to 0}\ln\gamma_2^{\infty} = A_{21} \qquad \text{Eq 10}$$

Table 7. Margules parameters obtained by $G^E/RTX_1X_2^2$ linear regression

System	Parameters		Linear regression
	A_{12}	A_{21}	R^2
Allyl Alcohol (1)/2-hexanol(2)	0.030	0.2224	0.9986
Allyl Alcohol (1)/MIBC(2)	0.0337	0.1341	0.9999
Allyl Alcohol (1)/2-hexanone(2)	0.2661	0.4213	0.9999
Allyl Alcohol (1) /MIBK(2)	0.2788	0.4039	0.9996
2-Hexanone (1)/2-hexanol(2)	0.1362	0.1124	0.9996
MIBK (1)/MIBC(2)	0.1223	0.1731	0.9997

As reported Kurihara et al [31], ε for isobaric systems can be large (as high as 0.04) and neglect it, is not recommended. Herington proposed an semi-empirical approach of this term by use of the total boiling range of the mixture [12] (Eq 11- 12), where γ_1 and γ_2 are the activity coefficients which were calculated by Eq 3, and A, B are the areas above and below of the abscissa axis in $Ln\left(\frac{\gamma_1}{\gamma_2}\right)$ vs x_1 (area test plot Figure S1). If deviation from experimental errors ($|D-J|$) are less than 10, the corresponding VLE data set can be judged as thermodynamically consistent.

$$D = 100\left|\frac{A-B}{A+B}\right| = 100\,\frac{\left|\int_0^1 Ln\left(\frac{\gamma_1}{\gamma_2}\right)dx_1\right|}{\int_0^1\left|Ln\left(\frac{\gamma_1}{\gamma_2}\right)\right|dx_1} \qquad \text{Eq 11}$$

$$J = 50\left|\frac{\Delta H_m}{\Delta G^E}\right|\left|\frac{T_{max}-T_{min}}{T_{min}}\right|, \qquad \left|\frac{\Delta H_m}{\Delta G_m^E}\right| = 3 \qquad \text{Eq 12}$$

Wisniak [13] slightly modified the Herington criteria; ΔH_m data were correlated against ΔG_m^E from experimental data with good results using the Eq 13. In this work, the data was calculated from

experiments, using Eq 3 - 4 and plotted in Figure 3. Each data set was correlated by a sixth order polynomial equation and the maximum value of excess free energy of mixing (ΔG_m^E) was calculated by derivation. ${}^{\Delta H_m}/_{\Delta G_m^E}$ Values were summarized in Table 8.

$$\Delta \mathrm{H_m}\ (\mathrm{J\ mol^{-1}}) = -237.02 + 1.3863\ \Delta G_m^E (\mathrm{J\ mol^{-1}}) \qquad \text{Eq 13}$$

The Van Ness method [14] is a suitable method for testing the sensitive to the selected model as well the reliability of VLE values, thought the mean absolute deviation between experimental data and calculated values by a given thermodynamic model[28]. It is defined by Eq 14 and Eq 15, where N mean the number of experimental points, P_i^{exp} and $\mathrm{y_i^{exp}}$ the experimental pressures and mole fraction in vapor phase, P_i^{cal} and $\mathrm{y_i^{cal}}$ the calculated values that obtained by UNIQUAC, NRTL, and WILSON thermodynamic models. As to the Van Ness method, VLE data can be considered thermodynamically consistent if Δy and ΔP values are less than 1.

$$\Delta \mathrm{y} = \frac{1}{\mathrm{N}} \sum_{\mathrm{i=1}}^{\mathrm{N}} 100 \left| \mathrm{y_i^{exp}} - \mathrm{y_i^{cal}} \right| \qquad \text{Eq 14}$$

$$\Delta P = \frac{1}{N} \sum_{i=1}^{N} 100 \left| \frac{P_i^{exp} - P_i^{cal}}{P_i^{exp}} \right| \qquad \text{Eq 15}$$

According with the obtained results given in Table 8, all binaries were found consistent with the Redlich Kister area test (|A*|<0.03), Aspen plus tool, Modified Herington test ($|D - J| < 10$) and Van Ness method (Δy < 1) and ΔT< 1). Despite the fact that the Herington test has been successfully implemented in similar systems containing non-polar compound and alcohols [13][32][33][34], in this study, from 6 data sets, only 2-hexanone (1)/2-hexanol (2) binary was found consistent $|D - J| = 0.99$. According to the literature, some researchers have also shown data sets that failed Herington test but passed Redlich-Kister area test [8][35][36]. In our case, this failure in the Herington test, has been also corrected by leaving out value of ${}^{\Delta H_m}/_{\Delta G_m^E} = 3$ (Wisniak criterion Eq 13).

Table 8. Results of Herington test and Van Ness Method for thermodynamic consistency check

System	$\left\lvert\frac{\Delta H_m}{\Delta G^E}\right\rvert$	Herington			Wisniak (Modified Herington)			Van Ness		Redlich-Kister total area test and Aspen tool	
		D	J	$\lvert D - J\rvert$	D	J[d]	$\lvert D - J\rvert$	Δy	${}^{\Delta P}/_{kPa}$	|A*|< 0.03	Result
Allyl Alcohol (1)/2-hexanol (2)	0.94	12.24	66.21	53.96	12.24	20.86	8.6	0.225[a] 0.259[b] 0.182[c]	0.024[a] 0.027[b] 0.045[c]	0.007	Passed
Allyl Alcohol (1)/MIBC(2)	1.89	24.88	54.04	29.16	24.88	34.09	9.21	0.043[a] 0.044[b]	0.054[a] 0.060[b]	0.010	Passed

								0.042[c]	0.053[c]		
Allyl Alcohol (1)/2-hexanone(2)	0.55	14.46	46.5	32.03	14.46	8.49	5.97	0.069[a] 0.067[b] 0.066[c]	0.035[a] 0.035[b] 0.035[c]	0.024	Passed
Allyl Alcohol (1)/MIBK(2)	0.51	2.90	29.4	26.46	2.90	4.95	2.04	0.109[a] 0.103[b] 0.106[c]	0.035[a] 0.038[b] 0.043[c]	0.0051	Passed
2-hexanone (1)/2-hexanol (2)	0.95	14.07	15.1	0.99	14.07	4.75	9.33	0.237[a] 0.238[b] 0.313[c]	0.034[a] 0.021[b] 0.040[c]	0.0081	Passed
MIBK (1)/MIBC(2)	0.58	0.83	20.6	19.76	0.83	3.98	3.16	0.276[a] 0.279[b] 0.279[c]	0.060[a] 0.060[b] 0.063[c]	0.0006	Passed

[a]UNIQUAC model, [b]NRTL model, [c]WILSON model, [d]J value corrected with $\frac{\Delta H_m}{\Delta G_m^E}$ experimental ratio.

Additionally to the requirements associated to the Gibbs-Duhem equation, consistency between the end-points of VLE data sets (i.e., mole fraction of 0 and 1) and the vapor pressures of pure components must be applied [15]. The pure component consistency test is presented in Eq 16 and Eq 17. Where p_1^0 and p_2^0 are the pure component vapor pressures, P_{bubble} is the bubble point pressure. Consistency test is passed if ΔP_1^0 and ΔP_2^0 are less than 1. As presented in Table 9, all the experimental data sets pass this criterion.

$$\Delta P_1^0 = \left| \frac{P_{bubble}(x_1 \to 1) - p_1^0}{p_1^0} \right| \quad \text{Eq 16}$$

$$\Delta P_2^0 = \left| \frac{P_{bubble}(x_1 \to 0) - p_2^0}{p_2^0} \right| \quad \text{Eq 17}$$

Table 9. Pure component consistency test

System	$100\Delta P_1^0$	$100\Delta P_2^0$
Allyl alcohol (1)/ 2-hexanol(2)	0.028	0.025
Allyl alcohol (1)/ MIBC(2)	0.101	0.023
Allyl alcohol (1)/ 2-hexanone(2)	0.028	0.011
Allyl alcohol (1)/ MIBK(2)	0.064	0.002
2-Hexanone (1)/ 2-hexanol(2)	0.039	0.025
MIBK (1)/ MIBC(2)	0.088	0.010

3.4. VLE data correlation

The measured data for all binary systems were correlated by three thermodynamic models, UNIQUAC, NRTL and Wilson, using Aspen plus V11 regression tool. The corresponding interaction parameters were obtained by minimizing the maximum likelihood objective function (OF), defined by Eq 18. This OF consist on the sum of differences of measured and predicted variables [11], where P and T are the equilibrium pressure and temperature, respectively; x_i and y_i the liquid and vapor mole fraction, respectively; N and σ are the number of data point and the standard deviation, respectively. According to Renon and Prausnitz [18], the non-randomness parameter (α_{ij}) was set at 0.3. Concerning the UNIQUAC model, volume (r) and area (q) parameters for each component are given in Table 10.

$$OF = \sum_{i=1}^{N}\left[\left(\frac{T_i^{exp} - T_i^{cal}}{\sigma^T}\right)^2 + \left(\frac{P_i^{exp} - P_i^{cal}}{\sigma^P}\right)^2 + \left(\frac{x_i^{exp} - x_i^{cal}}{\sigma^x}\right)^2 + \left(\frac{y_i^{exp} - y_i^{cal}}{\sigma^y}\right)^2\right] \quad \text{Eq 18}$$

Table 10. Structural parameters r and q for UNIQUAC model[a]

Component	r	q
Allyl Alcohol	2.550	2.300
2-Hexanol	4.970	4.084
2-Hexanone	4.597	3.956
MIBC	4.802	4.124
MIBK	4.596	3.952

[a]Taken from Aspen database

To evaluate the difference between the experimental data and the calculated results, the root-mean-square deviation (RMSD) of equilibrium temperature and composition was calculated, according to equations 19 and 20, respectively. The corresponding binary coefficients of the three thermodynamic models for the six systems and those of RMSD are given in Table 10. For all binary systems, one can observe that RMSD (T) and RMSD (y) values are less than 0.24 K and 0.0089, respectively, which indicates that all binary systems have been adjusted successfully by the three thermodynamic models.

$$RMSD(T_i) = \left(\frac{\sum_{i=1}^{N}(T_i^{exp} - T_i^{cal})^2}{N}\right)^{0.5} \quad \text{Eq 19}$$

$$RMSD(y_i) = \left(\frac{\sum_{i=1}^{N}(y_i^{exp} - y_i^{cal})^2}{N}\right)^{0.5} \quad \text{Eq 20}$$

Table 11. Binary interaction coefficients, root-mean-square (RMSD) deviations in the equilibrium temperature and vapor phase mole fraction for all binary systems using NRTL, Wilson and UNIQUAC models.

Model	a_{ij}	a_{ji}	b_{ij}/K	b_{ji}/K	α_{ij}	RMSD(T/K)	RMSD(y_i)
Allyl alcohol (1)/2-hexanol (2)							
UNIQUAC	1.633	-1.355	-706.241	559.315		0.08	0.0035
NRTL	-5.542	2.735	2562.090	-1337.130	0.3	0.09	0.0039
Wilson	-1.746	4.433	869.063	-2040.740		0.17	0.0031
Allyl alcohol (1)/MIBC (2)							
UNIQUAC	-0.350	0.566	168.175	-287.860		0.19	0.0006
NRTL	0.529	-0.999	47.204	200.140	0.3	0.22	0.0007
Wilson	1.472	-1.330	-438.203	319.939		0.19	0.0006
Allyl alcohol (1)/2-hexanone (2)							
UNIQUAC	-0.771	1.573	355.772	-737.781		0.11	0.0089
NRTL	2.879	-3.805	-893.591	1390.490	0.3	0.12	0.0086
Wilson	3.122	-2.030	-1176.060	617.432		0.11	0.0084
Allyl alcohol (1)/MIBK (2)							
UNIQUAC	0.075	-0.461	0.000	75.230		0.16	0.0016
NRTL	0.961	0.094	-60.732	-163.638	0.3	0.16	0.0015
Wilson	0.566	-2.065	-152.915	550.640		0.18	0.0016
2-hexanone (1)/2-hexanol (2)							
UNIQUAC	4.480	-6.101	-1677.110	2292.310		0.14	0.0033
NRTL	-15.091	20.676	5899.130	-8057.630	0.3	0.10	0.0033
Wilson	1.221	0.586	-752.332	-83.526		0.19	0.0042
MIBK (1)/MIBC (2)							
UNIQUAC	1.437	-1.244	-643.368	547.072		0.23	0.0040
NRTL	-5.239	4.375	2239.820	-1827.390	0.3	0.23	0.0040
Wilson	-1.666	1.954	712.607	-893.601		0.24	0.0040

The quality of regression could be also confirmed through the correlation of experimental and calculated activity coefficients at 101.kPa, since these last coefficients are determined on the basis of all parameters involves in the objective function (Eq 18). The experimental data and regression results obtained by UNIQUAC, NRTL and Wilson, for all binary systems are shown in Figure 4, 5 and 6. As shown, T_{xy} diagrams have been adjusted successfully in all composition range unlike experimental activity coefficients in the infinite dilution zones. The latter is caused by high uncertainties in the GC characterization at high (>0.9) and low (<0.1) mole fractions [26].

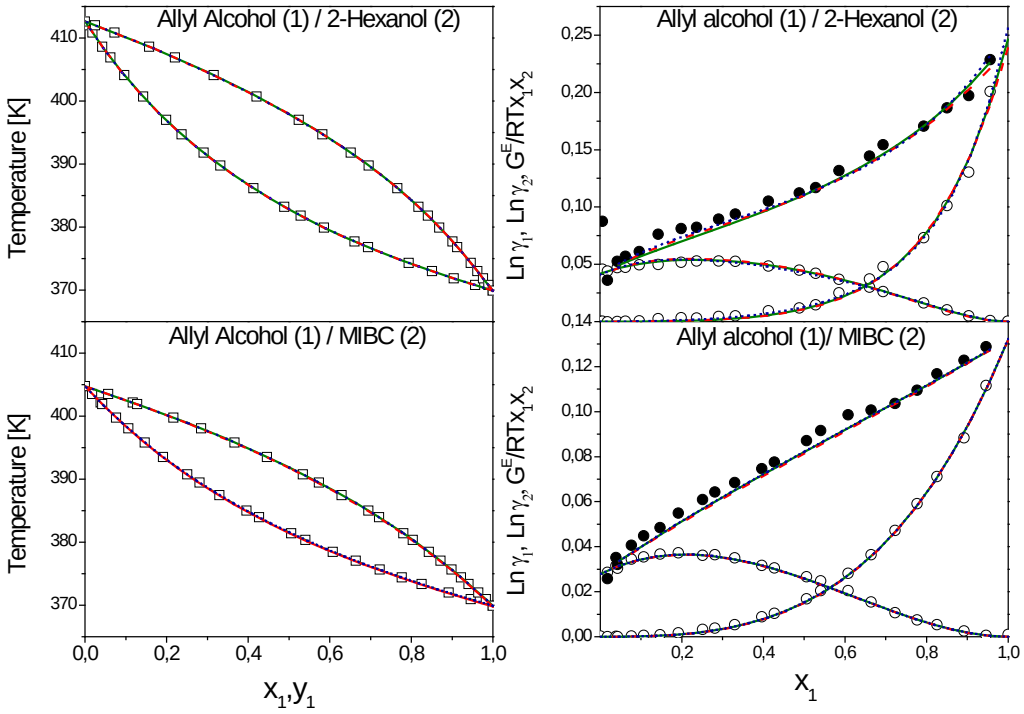

Figure 4. Phase diagram T_{xy} (left) and plot of Lnγ1, Lnγ2 and G^E/RTx_1x_2 vs x_1 at 101.13 kPa (right) for Allyl Alcohol/2-Hexanol and Allyl Alcohol/MIBC binaries. (□) Experimental data (○) Experimental Lnγ1, Lnγ2 (●) Experimental GE/RTx1x2. Green solid line, red dotted line and blue points correspond to UNIQUAC, NRTL and Wilson adjustment.

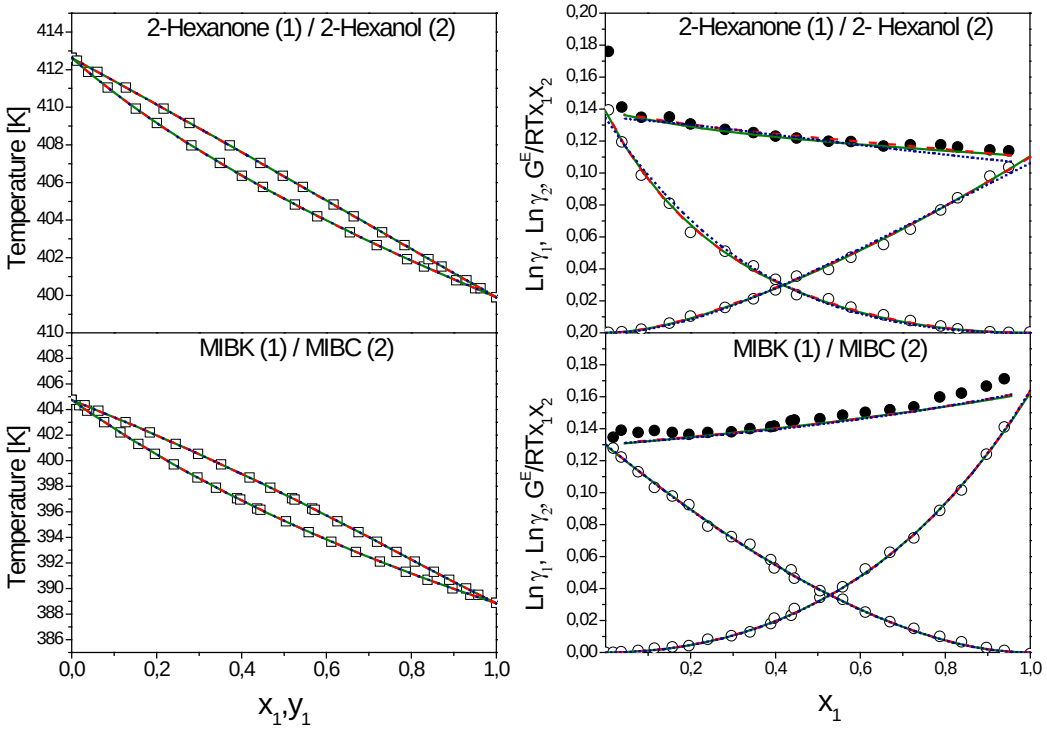

Figure 5. Phase diagram T_{xy} (left) and plot of Lnɣ1, Lnɣ2 and GE/RTx1x2 vs x1 at 101.13 kPa (right) for Allyl Alcohol/2-Hexanone and Allyl Alcohol/MIBK binaries. (□) Experimental data (○) Experimental Lnɣ1, Lnɣ2 (●) Experimental GE/RTx1x2. Green solid line, red dotted line and blue points correspond to UNIQUAC, NRTL and Wilson adjustment

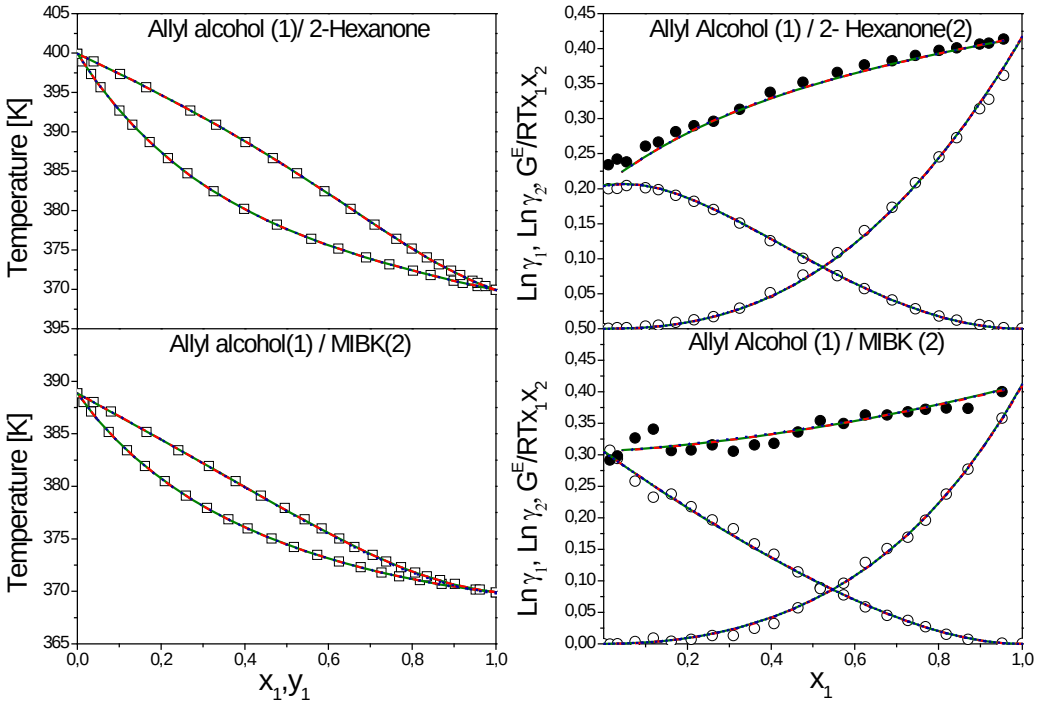

Figure 6. Phase diagram T_{xy} (left) and plot of $Ln\gamma_1$, $Ln\gamma_2$ and G^E/RTx_1x_2 vs x_1 at 101.13 kPa (right) for 2-Hexanone/2-Hexanone and MIBK/MIBC binaries. (□) Experimental data (○) Experimental $Ln\gamma_1$, $Ln\gamma_2$ (●) Experimental GE/RTx_1x_2. Green solid line, red dotted line and blue points correspond to UNIQUAC, NRTL and Wilson adjustment.

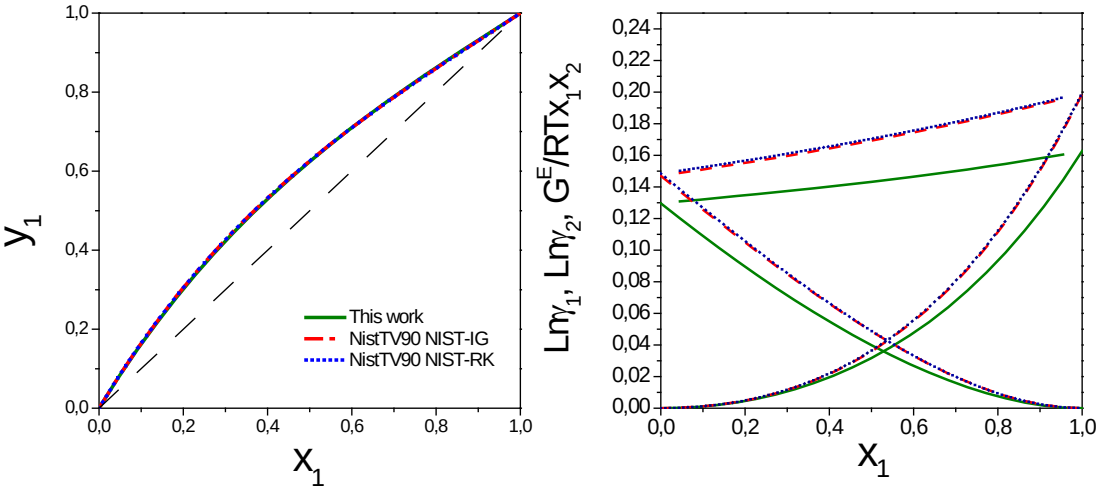

Figure 7. Diagram (x-y) (left) and plot of $Ln\gamma_1$, $Ln\gamma_2$ and G^E/RTx_1x_2 vs x_1 at 101.13 kPa (right) for MIBK/MIBC system. Green solid line, red dotted line and blue points correspond to simulated equilibrium using UNIQUAC parameters from this work and Aspen data based, respectively.

MIBK/MIBC system was compared with existing binary coefficients from the Aspen data based (NISTV90 NIST-IG and NISTV90 NIST-RK), using the UNIQUAC model. Figure 7 presents the phase equilibrium diagram x-y at 101.32 kPa and the correlation of the activity coefficients. As observed, this work agrees with the vapor-liquid distribution ratios (K-values), using UNIQUAC parameters from the Aspen data based. Nevertheless, a deviation in the activity coefficients has been identified. Hence,

considering that activity coefficients values at low pressures depends of K-values, system pressure and equilibrium temperature (Eq 3), this difference is possibly due to a slight shift in these parameters.

4. CONCLUSION

Isobaric vapor-liquid equilibrium (VLE) data for Allyl alcohol/2-hexanol, Allyl alcohol/2-hexanone, 2-hexanone/2-hexanol, Allyl alcohol/MIBC, Allyl alcohol/MIBK, and MIBK/MIBC systems were measured at 101.32 kPa. Non azeotrope was formed in these six binary systems and positive deviations from Raoul's law were found in all systems, following the order Allyl alcohol/2-hexanone > Allyl alcohol/MIBK > MIBK/MIBC > 2-hexanone/2-Hexanol >Allyl alcohol/2-Hexanol > Allyl alcohol/MIBC. Where Allyl alcohol/2-hexanone and Allyl alcohol/MIBK showed the biggest non-ideality compared to those of the other four mixtures. All measured VLE data sets passed the thermodynamic consistency with Herington (Wisniak criterion), Van Ness, pure component consistency and Redlich-Kister total area tests. Furthermore, all systems were successfully fitted by UNIQUAC, NRTL and Wilson thermodynamic models, and the corresponding binary coefficients were correlated. MIBK/MIBC system was compared with existing binary coefficients in Aspen data based (NISTV90 NIST-IG and NISTV90 NIST-RK), using UNIQUAC model.

5. REFERENCES

[1] S. Tazawa, N. Ota, M. Tamura, Y. Nakagawa, K. Okumura, and K. Tomishige, "Deoxydehydration with Molecular Hydrogen over Ceria-Supported Rhenium Catalyst with Gold Promoter," *ACS Catal.*, vol. 6, no. 10, pp. 6393–6397, 2016.

[2] L. Sandbrink, E. Klindtworth, H. U. Islam, A. M. Beale, and R. Palkovits, "ReOx/TiO2: A Recyclable Solid Catalyst for Deoxydehydration," *ACS Catal.*, vol. 6, no. 2, pp. 677–680, 2016.

[3] Y. Kon, M. Araque, T. Nakashima, S. Paul, F. Dumeignil, and B. Katryniok, "Direct Conversion of Glycerol to Allyl Alcohol Over Alumina-Supported Rhenium Oxide," *ChemistrySelect*, vol. 2, no. 30, pp. 9864–9868, 2017.

[4] K. Silva Vargas, M. Araque Marin, B. Katryniok, and M. Sadakane, "Deoxydehydration of glycerol to allyl alcohol catalyzed by ceria-supported oxide,"*submitted to Applied Catalyst A.*, 2020.

[5] V. Canale, L. Tonucci, M. Bressan, and N. D'Alessandro, "Deoxydehydration of glycerol to allyl alcohol catalyzed by rhenium derivatives," *Catal. Sci. Technol.*, vol. 4, no. 10, pp. 3697–3704, 2014.

[6] N. N. Tshibalonza and J. C. M. Monbaliu, "Revisiting the deoxydehydration of glycerol towards allyl alcohol under continuous-flow conditions," *Green Chem.*, vol. 19, no. 13, pp. 3006–3013, 2017.

[7] C. Boucher-Jacobs and K. M. Nicholas, "Catalytic deoxydehydration of glycols with alcohol reductants," *ChemSusChem*, vol. 6, no. 4, pp. 597–599, 2013.

[8] J. Duran, F. Cordoba, I. Gerardo Rodriguez, and A. Orjuela, "Vapor-liquid equilibrium of the ethanol + 3-methyl-1-butanol system at 50.66, 101.33 and 151.99 kPa," *Fluid Phase Equilib.*, p. 400, 2013.

[9] K. Moodley, M. Hussain, P. Naidoo, and T. Naidoo, "Isobaric Vapor-Liquid Equilibrium Data for Water (1) + 2-Methyl-propan-1-ol (2), 2-Methyl-propan-1-ol (1) + Pyridine (2), and Water (1) + 2-Methyl-propan-1-ol (2) + Pyridine (3) Systems," *J. Chem. Eng. Data*, vol. 65, no. 2, pp. 647–654, 2020.

[10] J. Li, C. Hua, S. Xiong, F. Bai, P. Lu, and J. Ye, "Vapor-Liquid Equilibrium for Binary Systems of Allyl Alcohol + Water and Allyl Alcohol + Benzene at 101.3 kPa," *J. Chem. Eng. Data*, vol. 62, no. 10, pp. 3004–3008, 2017.

[11] C. A. Sánchez, A. A. Herrera, J. C. Vargas, I. D. Gil, and G. Rodríguez, "Isobaric Vapor Liquid Equilibria for Binary Mixtures of Isoamyl Acetate + Ethyl Acetate at 50 and 100 kPa," *J. Chem. Eng. Data*, vol. 64, no. 5, pp. 2110–2115, 2019.

[12] E. Herington, "Tests for the consistency of experimental isobaric vapour-liquid equilibrium data," *J. Inst. Pet.*, vol. 37, p. 457−470, 1951.

[13] J. Wisniak, "The Herington Test for Thermodynamic Consistency," *Ind. Eng. Chem. Res.*, vol. 33, no. 1, pp. 177–180, 1994.

[14] H. C. Van Ness, S. M. Byer, and R. E. Gibbs, "Vapor-liquid equilibrium: Part I. An appraisal of data reduction methods," *AIChE J*, vol. 19, no. 2, pp. 238–244, 1973.

[15] J. W. Kang *et al.*, "Quality assessment algorithm for vapor-liquid equilibrium data," *J. Chem. Eng. Data*, vol. 55, no. 9, pp. 3631–3640, 2010.

[16] K. Kojima, M. H. Moon, and K. Ochi, “Thermodynamic consistency test of Vapor-liquid equilibrium data,” *J. Mol. Struc.*, vol. 56, pp. 269–284, 1990.

[17] D. S. Abrams and J. M. Prausnitz, “Statistical thermodynamics of liquid mixtures: A new expression for the excess Gibbs energy of partly or completely miscible systems,” *AIChE J.*, vol. 21, no. 1, pp. 116–128, 1975.

[18] H. Renon and J. M. Prausnitz, “Local Compositions in Thermodynamic Excess Functions for Liquid Mixtures,” *AIChE J*, vol. 14, no. 1, pp. 135–144, 10968.

[19] G. M. Wilson, “Vapor-Liquid Equilibrium. XI. A New Expression for the Excess Free Energy of Mixing,” *J. Am. Chem. Soc.*, vol. 86, no. 2, pp. 127–130, 1964.

[20] R. W. Grabner and C. W. Clump, “Liquid-Vapor Equilibrium and Heats of Vaporization of Allyl Alcohol-Water Mixtures,” *J. Chem. Eng. Data*, vol. 10, no. 1, pp. 13–16, 1965.

[21] B. Diao *et al.*, “Isobaric Vapor-Liquid Phase Equilibrium Measurements for Allyl Alcohol with Chloroform, Ethyl Acetate, and Methyl Propionate at 101.3 kPa,” *J. Chem. Eng. Data*, vol. 64, no. 2, pp. 682–687, 2019.

[22] Z. N. Esina, A. M. Miroshnikov, and M. R. Korchuganova, “Flash Points of Secondary Alcohol and n-Alkane Mixtures,” *J. Phys. Chem. B*, vol. 119, no. 46, pp. 14697–14704, 2015.

[23] F. Gharagheizi, “Determination of normal boiling vaporization enthalpy using a new molecular-based model,” *Fluid Phase Equilib.*, vol. 317, pp. 43–51, 2012.

[24] F. Mohammed, M. Qasim, A. A. Aidan, and N. A. Darwish, “Measurement and correlation of isobaric binary vapor-liquid equilibria for water and 2-propanol each with 1-butyl-1-methypyrrolidinium chloride and 1-butyl-1-methylpyrrolidinium tri fl uoromethanesulfonate,” *J. Mol. Liq.*, vol. 264, pp. 534–542, 2018.

[25] E. C. Voutsas, C. Pamouktsis, D. Argyris, and G. D. Pappa, “Measurements and thermodynamic modeling of the ethanol – water system with emphasis to the azeotropic region,” *Fluid Phase Equilib.*, vol. 308, no. 1–2, pp. 135–141, 2011.

[26] J. Wisniak and A. Apelblat, “An Assessment of Thermodynamic Consistency Tests for Vapor-Liquid equilibrium data,” *Phys. Chem. Liq.*, no. September, 1997.

[27] K. Liu *et al.*, “Vapour-liquid equilibrium measurements and correlation for separating azeotropic mixture (ethyl acetate + n-heptane) by extractive distillation,” *J. Chem. Thermodyn.*, vol. 144, p. 106075, 2020.

[28] Y. Ma, J. Gao, M. Li, Z. Zhu, and Y. Wang, “Isobaric vapour–liquid equilibrium measurements and extractive distillation process for the azeotrope of (N,N-dimethylisopropylamine + acetone),” *J. Chem. Thermodyn.*, vol. 122, pp. 154–161, 2018.

[29] J. Smith, H. Van Ness, and M. Abbott, *Introduction to Chemical Engineering Thermodynamics*, 7th editio. New York: McGraw-Hill, 2005.

[30] Aspen Technology Inc. and Aspen Plus V 8.4, “Aspen Physical Property System: Physical Property Methods,” *Methods*, pp. 1–234, 2013.

[31] K. Kurihara, Y. Egawa, K. Ochi, and K. Kojima, “Evaluation of thermodynamic consistency of isobaric and isothermal binary vapor-liquid equilibrium data using the PAI test,” *Fluid Phase Equilib.*, vol. 219, no. 1, pp. 75–85, 2004.

[32] M. Pradeep Kumar, S. Tasleem, and G. R. Kumar, “Isobaric vapor-liquid equilibrium data of 2-methyl-propan-2-ol (1) + heptan-1-ol (2), methanol (1) + heptan-1-ol (2), ethanol (1) + heptan-

1-ol (2), and propan-1-ol (1) + heptan-1-ol (2) at 96.5 kPa," *J. Chem. Eng. Data*, vol. 57, no. 11, pp. 3109–3113, 2012.

[33] Y. Zhang *et al.*, "Vapour–liquid equilibrium and extractive distillation for separation of azeotrope isopropyl alcohol and diisopropyl ether," *J. Chem. Thermodyn.*, vol. 131, pp. 294–302, 2019.

[34] Y. Gao *et al.*, "Measurement and Correlation of Isobaric Vapor-Liquid Equilibrium for Binary Systems of Allyl Alcohol with Isobutyl Acetate, Butyl Acetate, and Butyl Propionate at 101.3 kPa," *J. Chem. Eng. Data*, vol. 63, no. 3, pp. 845–852, 2018.

[35] H. Liu, X. Cui, Y. Zhang, T. Feng, and K. Zhang, "Isobaric Vapor-Liquid Equilibrium for the Binary and Ternary System with Isobutyl Alcohol, Isobutyl Acetate and Dimethyl Sulfoxide at 101.3 kPa," *J. Chem. Eng. Data*, vol. 62, no. 6, pp. 1902–1909, 2017.

[36] J. M. Resa, M. A. Betolaza, C. González, and A. Ruiz, "Isobaric vapor-liquid equilibria of acetone-propyl ether and isopropyl ether-propyl ether systems. Corroboration of no reverse volatility," *Fluid Phase Equilib.*, vol. 110, no. 1–2, pp. 205–217, 1995.

Supporting information

Isobaric Vapor-liquid equilibrium data for six binary systems: Allyl alcohol/2-hexanol, Allyl alcohol/2-hexanone, 2-hexanone/2-hexanol, Allyl alcohol/MIBC, Allyl alcohol/MIBK, and MIBK/MIBC at 101.32 kPa.

Karen Silva[1], Marcia Araque[1], Benjamin Katryniok[1]

[1] Univ. Lille, CNRS, Centrale Lille, ENSCL, Univ. Artois, UMR 8181 - UCCS - Unité de Catalyse et Chimie du Solide, F-59000 Lille, France

Supporting Information contains: 1 pages, and 1 figure

Figure S1

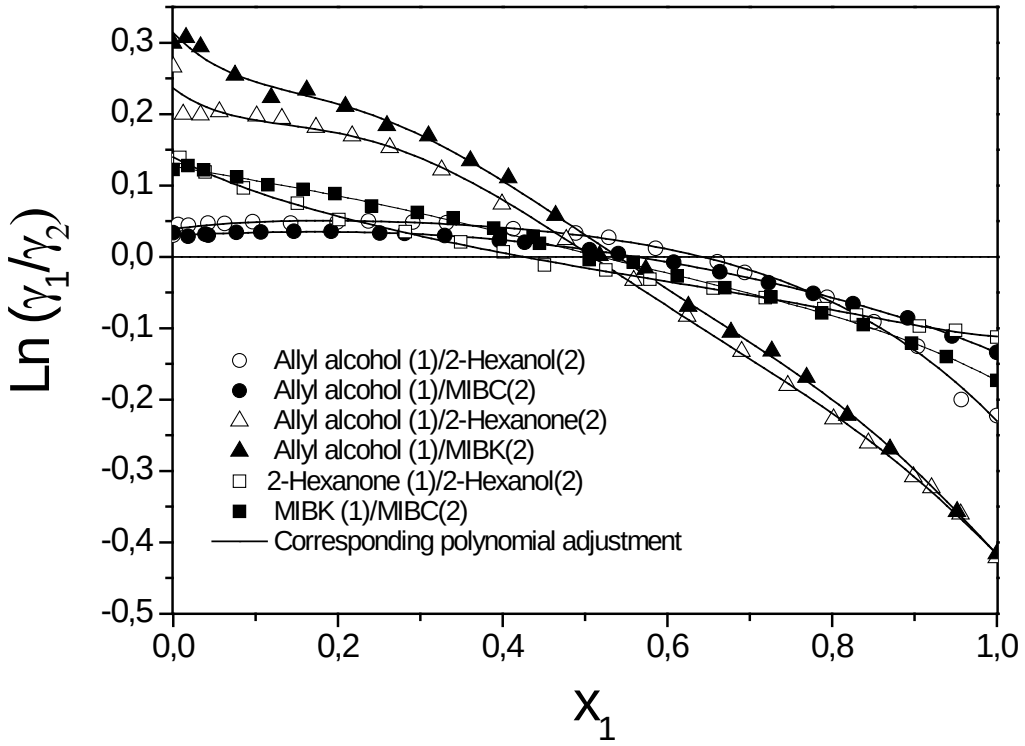

Figure S1. Ln ($\gamma_{1/}\gamma_{2)}$ vs x_1 plot of all binary systems, used in the thermodynamic consistency tests based on Gibbs-Duhem equation.